Journal of Sound and Vibration (1997) **203**(4), 707–716

LETTERS TO THE EDITOR

SIMULTANEOUS FORWARD AND BACKWARD WHIRLING IN A JEFFCOTT ROTOR SUPPORTED ON DISSIMILAR HYDRODYNAMIC BEARINGS

C. Rao, R. B. Bhat and G. D. Xistris

Department of Mechanical Engineering, Concordia University, 1455 De Maisonneuve Blvd. West, Montreal, Quebec, H3G 1M8, Canada

(*Received* 21 *December* 1995, *and in final form* 11 *October* 1996)

1. INTRODUCTION

A Jeffcott rotor supported on identical fluid film bearings causes the disk to whirl in the backward sense for a speed range in between the critical speeds [1–7]. Rajalingham *et al*. [8] showed that as the disk whirls in the backward sense in between the critical speeds, the journal continues to whirl in the forward sense. The backward whirl commences at the disk and as the speed increases, it extends over a certain central portion of the shaft and then shrinks back towards the disk before disappearing. Studies using the stiffness and damping characteristics of the supporting hydrodynamic bearings, showed that the combined influence of the stiffness asymmetry and the damping could suppress the occurrence of the backward whirling, when the flexibility of the rotor is sufficiently small [6]. Further, the backward whirling of the disk could be eliminated either by increasing the slenderness ratio of the bearings or the viscosity of the lubricant, or by reducing the clearance ratio of the bearings. The phenomenon of simultaneous forward and backward whirling in a Jeffcott rotor with an identical bearing was experimentally verified by Rao *et al*. [9].

The phenomenon of simultaneous forward and backward whirling motions in a Jeffcott rotor supported on two dissimilar bearings is studied in the present analysis. The dissimilarities may have been introduced in the design itself in the form of different loads on the two bearings or different bearing geometries. Moreover, even if the two bearings are identical by design, the manufacturing precision, wear, variation in lubricant flow rate and oil temperature could introduce dissimilarity in the bearings. The equations of motion of the disk are derived using the influence coefficient method and the force balance at the journal is used to formulate the remaining governing equations. Euler-Bernoulli beam theory is used to obtain the necessary influence coefficients associated with the displacement and rotation components at the disk location. Gyroscopic couples are also considered in the analysis. The solution for imbalance response is determined by solving the resulting system of linear equations numerically.

2. ANALYSIS

2.1. *Equations of motion*

A schematic representation of a typical single mass rotor supported on dissimilar hydrodynamic bearings at the two ends is shown in Figure 1. The force and moment component on this rotor is also shown in the figure. The bending moments at a distance z along the rotor shaft is expressed as

$$EI\frac{\mathrm{d}^2\xi_x}{\mathrm{d}z^2} = -\left(\frac{1}{2}P_x - \frac{1}{l}G_x\right)z + P_x\left[z-\frac{l}{2}\right]^1 - G_x\left[z-\frac{l}{2}\right]^0, \tag{1}$$

0022–460X/97/240707 + 10 $25.00/0/sv960815

where ξ_x is the deflection along X and terms within the square brackets [] are considered only when the quantity inside is positive. A similar equation can be written for deflection ξ_y in the Y direction. The expression for the force components P_x, P_y and the moment components G_x, G_y at the disk location are given by

$$P_x = M\omega^2\delta_c \cos \omega t - M\ddot{\xi}_{xc} + Mg, \qquad P_y = M\omega^2\delta_c \sin \omega t - M\ddot{\xi}_{yc}, \tag{2, 3}$$

$$G_x = -J\omega\dot{\theta}_{yc}, \qquad G_y = J\omega\dot{\theta}_{xc}. \tag{4, 5}$$

The integration of equation (1) using the boundary conditions $\xi_x = \xi_{xl}$ at $z = 0$, $\xi_x = \xi_{xr}$ at $z = l$, $\xi_x = \xi_{xc}$ at $z = l/2$ and $\mathrm{d}\xi_x/\mathrm{d}z = \theta_{xc}$ at $z = l/2$ results in the following equations:

$$EI(2\xi_{xc} - \xi_{xr} - \xi_{xl}) = \tfrac{1}{24}P_x l^3, \qquad EI(\theta_{xc} - (\xi_{xr} - \xi_{xl})/l) = -\tfrac{1}{12}G_x l. \tag{6, 7}$$

Similarly for the y-z plane, the governing equations can be expressed as

$$EI(2\xi_{yc} - \xi_{yr} - \xi_{yl}) = \tfrac{1}{24}P_y l^3, \qquad EI(\theta_{yc} - (\xi_{yr} - \xi_{yl})/l) = \tfrac{1}{12}G_y l. \tag{8, 9}$$

Substituting the expressions for the force components P_x, P_y and moment components G_x, G_y from equations (2–5) into equations (6–9) results in

$$(2\xi_{xc} - \xi_{xr} - \xi_{xl}) = (2\mu_s/\omega_0^2)(\omega^2\delta_c \cos \omega t - \ddot{\xi}_{xc} + g), \tag{10}$$

$$(2\xi_{yc} - \xi_{yr} - \xi_{yl}) = (2\mu_s/\omega_0^2)(\omega^2\delta_c \sin \omega t - \ddot{\xi}_{yc}), \tag{11}$$

$$(\theta_{xc} - (\xi_{xr} - \xi_{xl})/l) = -(4\bar{J}/\omega_s)(\omega\dot{\theta}_{yc}), \tag{12}$$

$$(\theta_{yc} - (\xi_{yr} - \xi_{yl}/l) = (4\bar{J}/\omega_s)(\omega\dot{\theta}_{xc}). \tag{13}$$

Equations (10–13) can be written in non-dimensional form as

$$2(\omega^2/\omega_s^2)\overline{\xi}''_{xc} + 2\overline{\xi}_{xc} - \bar{c}_r\overline{\xi}_{xr} - \bar{c}_l\overline{\xi}_{xl} = 2(\omega^2/\omega_s^2)\overline{\delta}_c \cos \omega t, \tag{14}$$

$$2(\omega^2/\omega_s^2)\overline{\xi}''_{yc} + 2\overline{\xi}_{yc} - \bar{c}_r\overline{\xi}_{yr} - \bar{c}_l\overline{\xi}_{yl} = 2(\omega^2/\omega_s^2)\overline{\delta}_c \sin \omega t, \tag{15}$$

$$\overline{\theta}_{xc} - \bar{c}_r\overline{\xi}_{xr} + \bar{c}_l\overline{\xi}_{xl} = -4\bar{J}(\omega^2/\omega_s^2)\overline{\theta}'_{yc}, \tag{16}$$

$$\overline{\theta}_{yc} - \bar{c}_r\overline{\xi}_{yr} + \bar{c}_l\overline{\xi}_{yl} = 4\bar{J}(\omega^2/\omega_s^2)\overline{\theta}'_{xc}. \tag{17}$$

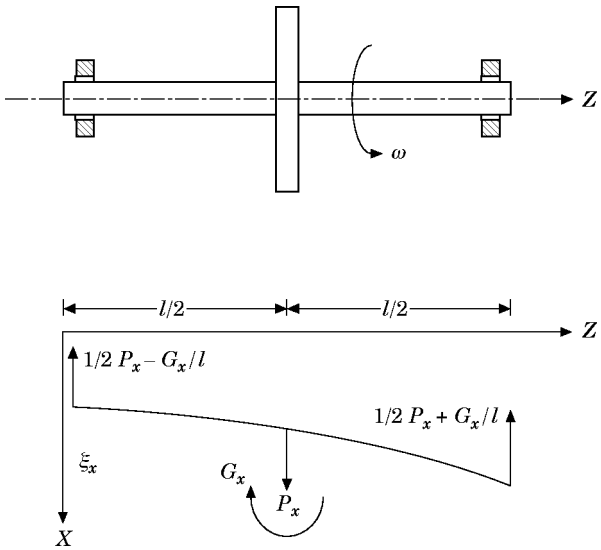

Figure 1. Bending moment diagram for X–Z plane.

2.2. *Force balance at the bearing*

The force balance at the bearings is expressed as follows:

$$\tfrac{1}{2}P_x - G_x/l - W/2 = K_{xx,l}\xi_{xl} + K_{xy,l}\xi_{yl} + C_{xx,l}\dot{\xi}_{xl} + C_{xy,l}\dot{\xi}_{yl}, \tag{18}$$

$$\tfrac{1}{2}P_y - G_y/l = K_{yx,l}\xi_{xl} + K_{yy,l}\xi_{yl} + C_{yx,l}\dot{\xi}_{xl} + C_{yy,l}\dot{\xi}_{yl}, \tag{19}$$

$$\tfrac{1}{2}P_x + G_x/l - W/2 = K_{xx,r}\xi_{xr} + K_{xy,r}\xi_{yr} + C_{xx,r}\dot{\xi}_{xr} + C_{xy,r}\dot{\xi}_{yr}, \tag{20}$$

$$\tfrac{1}{2}P_y - G_y/l = K_{yx,r}\xi_{xr} + K_{yy,r}\xi_{yr} + C_{yx,r}\dot{\xi}_{xr} + C_{yy,r}\dot{\xi}_{yr}. \tag{21}$$

Substituting the force component terms P_x and P_y from equations (6) and (7) in equations (18) and (19), moment components G_x from equation (8) and G_y from equation (9) in equation (20) and (21), and using the non-dimensional stiffness and damping coefficients results in

$$2(\overline{\xi}_{xc} - \bar{c}_l\overline{\xi}_{xl}) - \overline{\theta}_{xc} = 2\mu_s(\overline{K}_{xx,l}\overline{\xi}_{xl} + \overline{K}_{xy,l}\overline{\xi}_{yl}) + 2\mu_s(\overline{C}_{xx,l}\overline{\xi}'_{xl} + \overline{C}_{xy,l}\overline{\xi}'_{yl}), \tag{22}$$

$$2(\overline{\xi}_{yc} - \bar{c}_l\overline{\xi}_{yl}) - \overline{\theta}_{yc} = 2\mu_s(\overline{K}_{yx,l}\overline{\xi}_{xl} + \overline{K}_{yy,l}\overline{\xi}_{yl}) + 2\mu_s(\overline{C}_{yx,l}\overline{\xi}'_{xl} + \overline{C}_{yy,l}\overline{\xi}'_{yl}), \tag{23}$$

$$2(\overline{\xi}_{xc} - \bar{c}_r\overline{\xi}_{xr}) + \overline{\theta}_{xc} = 2\mu_s(\overline{K}_{xx,r}\overline{\xi}_{xr} + \overline{K}_{xy,r}\overline{\xi}_{yr}) + 2\mu_s(\overline{C}_{xx,r}\overline{\xi}'_{xr} + \overline{C}_{xy,r}\overline{\xi}'_{yr}), \tag{24}$$

$$2(\overline{\xi}_{yc} - \bar{c}_r\overline{\xi}_{yr}) + \overline{\theta}_{yc} = 2\mu_s(\overline{K}_{yx,l}\overline{\xi}_{xl} + \overline{K}_{yy,l}\overline{\xi}_{yl}) + 2\mu_s(\overline{C}_{yx,r}\overline{\xi}'_{xr} + \overline{C}_{yy,r}\overline{\xi}'_{yr}). \tag{25}$$

2.3. *Imbalance whirling motion*

Under steady state conditions the imbalance response can be expressed as follows:

$$\begin{aligned}
\overline{\xi}_{xl} &= (\delta_c/c)(a_{xl}\cos\omega t + b_{xl}\sin\omega t), & \overline{\xi}_{xr} &= (\delta_c/c)(a_{xr}\cos\omega t + b_{xr}\sin\omega t),\\
\overline{\xi}_{yl} &= (\delta_c/c)(a_{yl}\cos\omega t + b_{yl}\sin\omega t), & \overline{\xi}_{yr} &= (\delta_c/c)(a_{yr}\cos\omega t + b_{yr}\sin\omega t),\\
\overline{\xi}_{xc} &= (\delta_c/c)(a_{xc}\cos\omega t + b_{xc}\sin\omega t), & \overline{\xi}_{yc} &= (\delta_c/c)(a_{yc}\cos\omega t + b_{yc}\sin\omega t),\\
\overline{\theta}_{xc} &= (\delta_c/c)(c_{xc}\cos\omega t + d_{xc}\sin\omega t), & \overline{\theta}_{yc} &= (\delta_c/c)(c_{yc}\cos\omega t + d_{yc}\sin\omega t).
\end{aligned} \tag{26}$$

Substituting the steady state solution in equation (26) into the equation of motion and equating the $\cos\omega t$ and $\sin\omega t$ terms from the left and right sides of equations (14–17) results in

$$2a_{xc}(1 - \omega^2/\omega_s^2) - \bar{c}_r a_{xr} - \bar{c}_l a_{xl} = 2(\omega^2/\omega_s^2), \tag{27}$$

$$2b_{xc}(1 - \omega^2/\omega_s^2) - \bar{c}_r b_{xr} - \bar{c}_l b_{xl} = 0, \tag{28}$$

$$2a_{yc}(1 - \omega^2/\omega_s^2) - \bar{c}_r a_{yr} - \bar{c}_l a_{yl} = 0, \tag{29}$$

$$2b_{yc}(1 - \omega^2/\omega_s^2) - \bar{c}_r b_{yr} - \bar{c}_l b_{yl} = 2(\omega^2/\omega_s^2), \tag{30}$$

$$c_{xc} - \bar{c}_r a_{xr} + \bar{c}_l a_{xl} = -4\bar{J}(\omega^2/\omega_s^2)d_{yc}, \qquad d_{xc} - \bar{c}_r b_{xr} + \bar{c}_l b_{xl} = 4\bar{J}(\omega^2/\omega_s^2)c_{yc}, \tag{31, 32}$$

$$c_{yc} - \bar{c}_r a_{yr} + \bar{c}_l a_{yl} = 4\bar{J}(\omega^2/\omega_s^2)d_{xc}, \qquad d_{yc} - \bar{c}_r b_{yr} + \bar{c}_l b_{yl} = -4\bar{J}(\omega^2/\omega_s^2)c_{xc}. \tag{33, 34}$$

Similarly, the substitution of equation (26) in the equation of force balance at the bearing and equating $\cos\omega t$ and $\sin\omega t$ terms in equations (22–25) results in

$$2a_{xc} - 2\bar{c}_l a_{xl} - c_{xc} = 2\mu_s\overline{K}_{xx,l}a_{xl} + 2\mu_s\overline{K}_{xy,l}a_{yl} + 2\mu_s\overline{C}_{xx,l}b_{xl} + 2\mu_s\overline{C}_{xy,l}b_{yl}, \tag{35}$$

$$2b_{xc} - 2\bar{c}_l b_{xl} - d_{xc} = 2\mu_s\overline{K}_{xx,l}b_{xl} + 2\mu_s\overline{K}_{xy,l}b_{yl} - 2\mu_s\overline{C}_{xx,l}a_{xl} - 2\mu_s\overline{C}_{xy}a_{yl}, \tag{36}$$

$$2a_{yc} - 2\bar{c}_l a_{yl} - c_{xc} = 2\mu_s\overline{K}_{yx,l}a_{xl} + 2\mu_s\overline{K}_{yy,l}a_{yl} + 2\mu_s\overline{C}_{yx,l}b_{xl} + 2\mu_s\overline{C}_{yy,l}b_{yl}, \tag{37}$$

$$2b_{yc} - 2\bar{c}_l b_{yl} - d_{yc} = 2\mu_s\overline{K}_{yx,l}b_{xl} + 2\mu_s\overline{K}_{yy,l}b_{yl} - 2\mu_s\overline{C}_{yx,l}a_{xl} - 2\mu_s\overline{C}_{yy,l}a_{yl}, \tag{38}$$

TABLE 1

Data for computation

Disk mass (kg)	11
Type of bearings	Plain cylindrical
Bearing diameter (m)	0·0254
Bearing L/D ratio	1
Modulus of elasticity of the material of shaft	$2{\cdot}15 \times 10^{11}$
Viscosity of oil (Ns/m^2)	0·0241
Length of the rotor (m)	0·5105
Disk diameter (m)	0·2032
Shaft diameter (m)	0·022

$$2a_{xc} - 2\bar{c}_r a_{xr} + c_{xc} = 2\mu_s \bar{K}_{xx,r} a_{xr} + 2\mu_s \bar{K}_{xy,r} a_{yr} + 2\mu_s \bar{C}_{xx,r} b_{xr} + 2\mu_s \bar{C}_{xy,r} b_{yr}, \tag{39}$$

$$2b_{xc} - 2\bar{c}_r b_{xr} + d_{xc} = 2\mu_s \bar{K}_{xx,r} b_{xr} + 2\mu_s \bar{K}_{xy,r} b_{yl} - 2\mu_s \bar{C}_{xx,r} a_{xr} - 2\mu_s \bar{C}_{xy,r} a_{yr}, \tag{40}$$

$$2a_{yc} - 2\bar{c}_r a_{yr} + c_{xc} = 2\mu_s \bar{K}_{yx,r} a_{xr} + 2\mu_s \bar{K}_{yy,r} a_{yr} + 2\mu_s \bar{C}_{yx,r} b_{xr} + 2\mu_s \bar{C}_{yy,r} b_{yr}, \tag{41}$$

$$2b_{yc} - 2\bar{c}_r b_{yr} + d_{yc} = 2\mu_s \bar{K}_{yx,r} b_{xr} + 2\mu_s \bar{K}_{yy,r} b_{yr} - 2\mu_s \bar{C}_{yx,r} a_{xr} - 2\mu_s \bar{C}_{yy,r} a_{yr}. \tag{42}$$

The imbalance response, $\bar{R}$, is given by

$$\bar{R} = \bar{\xi}_{xl} + \mathrm{i}\bar{\xi}_{yl}, \quad \text{at left bearing;} \qquad \bar{R} = \bar{\xi}_{xr} + \mathrm{i}\xi_{yr}, \quad \text{at right bearing;}$$

$$\bar{R} = \bar{\xi}_{xc} + \mathrm{i}\bar{\xi}_{yc}, \quad \text{at disk.} \tag{43}$$

3. RESULTS AND DISCUSSION

The system of equations (27–42) describes the behaviour of a single mass rotor system with dissimilar bearings. A typical single mass rotor, whose details are given in Table 1 is analyzed using these equations. The imbalance response $\bar{R}$ of the rotor can be calculated, thus using the computed value of coefficients $a_{xl}, \ldots, c_{dc}$ in equation (26). The parameter $\delta_c = (c_l - c_r)/c$, where $c = (c_r + c_l)/2$, is used to express the dissimilarity of the end bearings in non-dimensional form for unequal support bearing clearances. The area of the elliptic orbit at the left bearing is evaluated from the expression $\pi\delta_c^2(a_{xl}b_{yl} - b_{xl}a_{yl})$ [9]. When the sign of this expression is positive, the whirl is forward and when it is negative, the whirl is backward.

Similarly, the sense of whirling motion at the right bearing and the disk location are evaluated from the area of the respective elliptical orbits, $\pi\delta_c^2(a_{xr}b_{yr} - b_{xr}a_{yr})$ and $\pi\delta_c^2(a_{xc}b_{yc} - b_{xc}a_{yc})$ [9]. Once again the positive or negative sign of the area determines whether the whirl is forward or backward.

The Ocvirk's short bearing theory and Sommerfeld's long bearing analysis are applied to find an approximate solution to Reynolds equation. The solution is approximated using one-dimensional analysis and later with a two-dimensional approach to obtain the actual pressure distribution. The Reynolds equations thus derived for the bearings are modelled as grid mesh points with the dependent variables θ and $\bar{z}$ represented by a finite number of points located at the intersections of the grid and are solved by the finite difference method to get the pressure field. This pressure field is integrated over the entire film domain and the fluid-film reaction forces and moments of these forces are obtained. The stiffness and damping coefficients of the fluid film in the bearings are determined [10].

Dissimilarity may arise in bearings for any one or all of the reasons together as described in the introduction. This affects the Sommerfeld number and in turn, the stiffness and

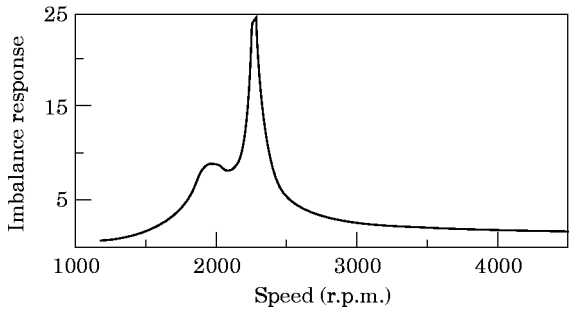

Figure 2. Imbalance response, $\bar{R}$, at the disk: load parameter $So_0 = 3{\cdot}0$, flexibility parameter $\mu_s = 2{\cdot}0$ and dissimilarity parameter $\delta = 0$.

damping coefficients in the hydrodynamic bearings. In the present study, dissimilarity is introduced by changing the bearing clearances which changes the Sommerfeld number. Considering a rotor model supported on identical bearings i.e., keeping the dissimilarity parameter $\delta = 0$, the load parameter So_0 and flexibility parameter μ_s are varied such that the rotor exhibits split criticals. For the value of $So_0 = 3{\cdot}0$ and $\mu_s = 2{\cdot}0$, the rotor exhibits split criticals, the first minor critical speed at 1900 r.p.m. and the second major critical speed at 2400 r.p.m. as shown in Figure 2. The area of the whirl orbit remains positive at the supporting bearings, indicating a forward whirling motion as shown in Figure 3. The area of the whirl orbit at the disk goes negative between the two critical speeds, indicating the simultaneous existence of forward whirling motion at the bearings and backward whirling motion at the disk as shown in Figure 4. Response at the bearing location is shown in Figure 5. Response at the right and left bearings are equal since the dissimilarity parameter is taken to be zero. Keeping the load parameter So_0 and flexibility

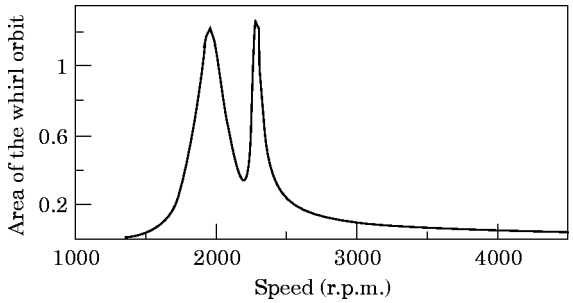

Figure 3. Area $\bar{A}$ of the whirl orbit at the bearing location: $So_0 = 3{\cdot}0$, $\mu_s = 2{\cdot}0$ and $\delta = 0$; ——, left bearing; – – –, right bearing.

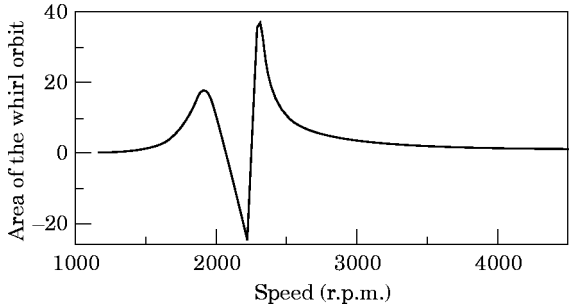

Figure 4. Area $\bar{A}$ of the whirl orbit at the disk: $So_0 = 3{\cdot}0$, $\mu_s = 2{\cdot}0$ and $\delta = 0$.

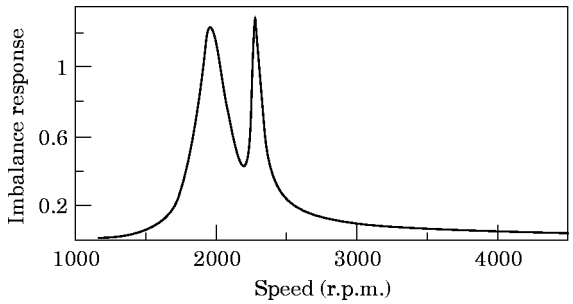

Figure 5. Imbalance response $\bar{R}$ at the bearing location: $So_0 = 3{\cdot}0$, $\mu_s = 2{\cdot}0$ and $\delta = 0$; ——, left bearing; – – –, right bearing.

parameter μ_s the same at 3·0 and 2·0, dissimilarity in the supporting bearing is introduced in the form of a dissimilarity parameter δ. Change in the dissimilarity parameter to a smaller value does not considerably affect the response at the disk and area of the whirl orbit. Varying the dissimilarity parameter to a value of 0·05 results in an increase of peak amplitude of response at the disk, however, the critical speed peaks shift towards the lower rotor speeds as shown in Figure 6. The same trend is observed in the area of the orbit at the disk and existence of the backward whirling motion for a range in between the two critical speeds at the disk is verified in Figure 7. The peak amplitude at the right bearing drops down considerably compared to the left bearing as depicted in Figure 8. However, the area of the whirl orbit at the bearing location remains positive as shown in Figure 9, indicating that the sense of whirl remains forward. The effect of increasing the dissimilarity factor further to a value of 0·1 results in critical speed peaks falling down to 1700 and 2000 r.p.m. at the rotor, with the increase in peak amplitude of response at the disk as observed in Figures 10 and 11. Response at the right bearing drops down drastically with

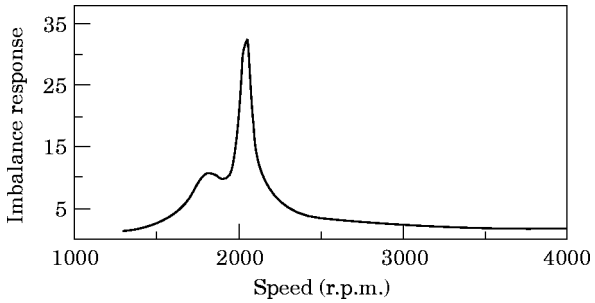

Figure 6. Imbalance response, $\bar{R}$, at the disk: load parameter $So_0 = 3{\cdot}0$, flexibility parameter $\mu_s = 2{\cdot}0$ and dissimilarity parameter $\delta = 0{\cdot}05$.

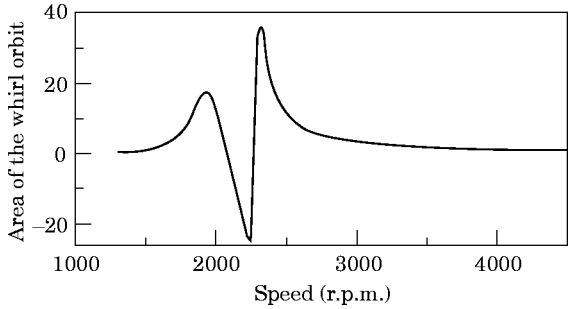

Figure 7. Area $\bar{A}$ of the whirl orbit at the disk: $So_0 = 3{\cdot}0$, $\mu_s = 2{\cdot}0$ and $\delta = 0{\cdot}05$.

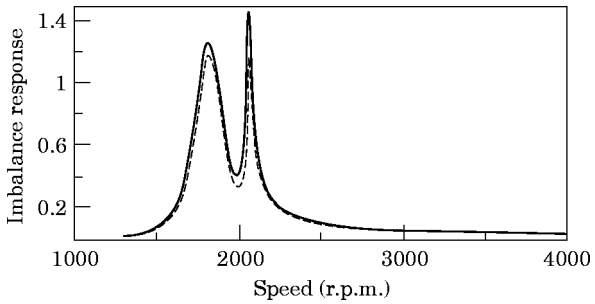

Figure 8. Imbalance response, $\bar{R}$, at the bearing location: $So_0 = 3{\cdot}0$, $\mu_s = 2{\cdot}0$ and $\delta = 0{\cdot}05$; ——, left bearing; – – –; right bearing.

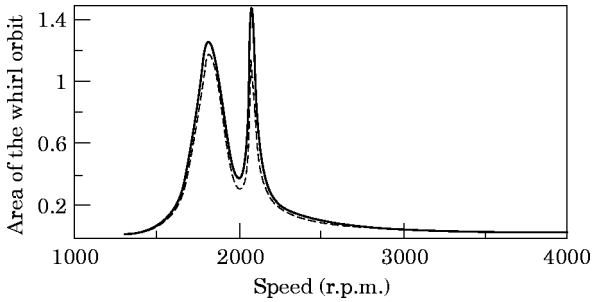

Figure 9. Area $\bar{A}$ of the whirl orbit at the bearing location, $So_0 = 3{\cdot}0$, $\mu_s = 2{\cdot}0$ and $\delta = 0{\cdot}05$; ——; left bearing; – – –, right bearing.

the peak amplitude of response for the second critical speed being smaller than the first one. At the left bearing location, the peak amplitude of response for the first critical speed was observed to drop down compared to the second critical speed, with the increase in dissimilarity parameter δ as depicted in Figure 12. The corresponding area of the whirl orbit remains positive at bearing locations indicating a forward whirl as shown in Figure 13. Increasing the value of δ to a value more than 1·0, the response at the disk and bearings does not follow the regular trend and the rotor becomes highly unstable.

The orbital diagram for the rotor with system parameters, $So_0 = 3{\cdot}0$ and $\mu_s = 2{\cdot}0$ and dissimilarity parameter $\delta = 0{\cdot}1$ are studied, because the rotor exhibits split criticals and hence the whirl patterns of the system at different rotor speeds are of interest. The orbital diagrams provide the amplitude and direction of whirl orbit, indicating whether the whirling motion is forward or backward at any defined location of the rotor system. The orbital diagram for the rotor resulting from the unbalance response is shown in Figure 14,

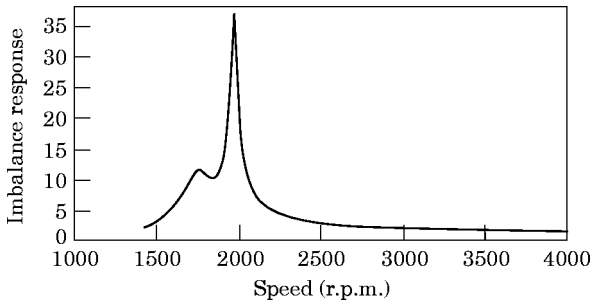

Figure 10. Imbalance response, $\bar{R}$, at the disk: load parameter $So_0 = 3{\cdot}0$, flexibility parameter $\mu_s = 2{\cdot}0$ and dissimilarity parameter $\delta = 0{\cdot}1$.

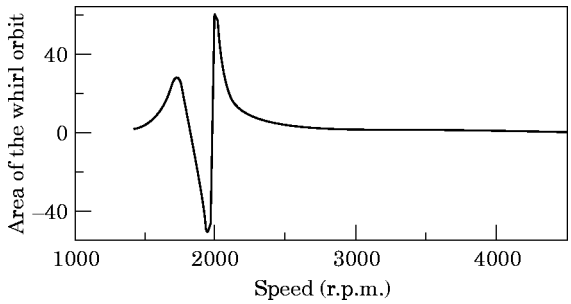

Figure 11. Area $\bar{A}$ of the whirl orbit at the disk: $So_0 = 3{\cdot}0$, $\mu_s = 2{\cdot}0$ and $\delta = 0{\cdot}1$.

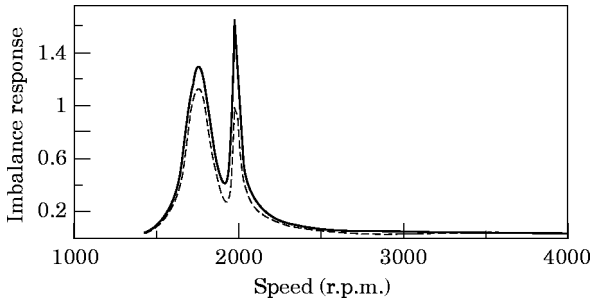

Figure 12. Imbalance response, $\bar{R}$, at the bearing location: $So_0 = 3{\cdot}0$, $\mu_s = 2{\cdot}0$ and $\delta = 0{\cdot}1$; ——, left bearing; – – –, right bearing.

for different locations in the shaft for a rotor speed of 2300 r.p.m. In Figure 14, $z/l = 0$ represents the orbit of the journal at the left bearing. Similarly, for $z/l = 0$–$0{\cdot}3$ the whirling motion is forward in the vicinity of the left bearing. At the point of transition from forward to backward whirling, when $z/l = 0{\cdot}30$, the whirl orbit becomes a straight line. The point of transition from forward to backward whirl occurs at a point on the rotor much in advance of that in the case of identical bearings [8]. This is due to variation in flexibility and load parameter and also due to the introduction of dissimilarity in the bearings.

4. CONCLUSIONS

Existence of the simultaneous forward and backward whirling motion at the disk location is verified for a rotor supported on dissimilar bearings. Effect of dissimilarity affects the peak amplitude of response and the critical speed peaks shifts towards the lower speed of the rotor. Change in the dissimilarity parameter does affect the imbalance

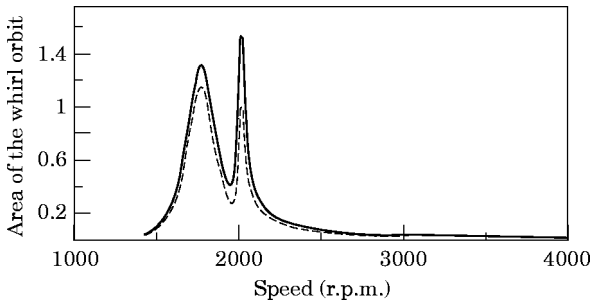

Figue 13. Area $\bar{A}$ of the whirl orbit at the bearing location, $So_0 = 3{\cdot}0$, $\mu_s = 2{\cdot}0$ and $\delta = 0{\cdot}1$; ——; left bearing; – – –, right bearing.

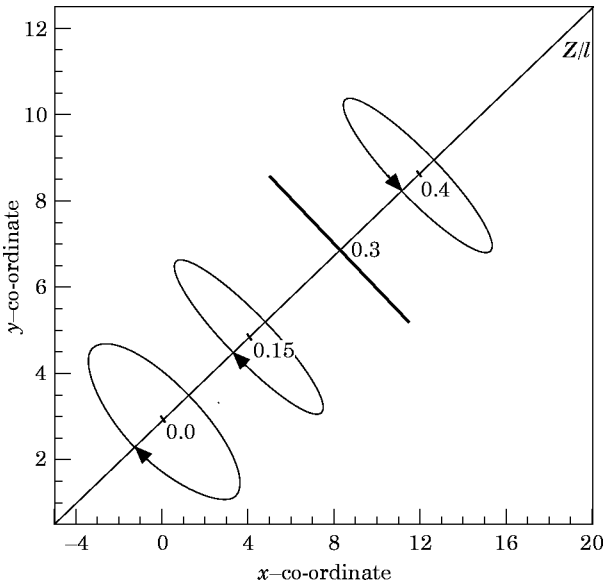

Figure 14. Non-dimensional imbalance orbit of the rotor, $So_0 = 3{\cdot}0$, $\mu_s = 2{\cdot}0$.

response at the bearings, with the peak amplitude of response at one bearing dropping down considerably compared to that at the other bearing. Simultaneous forward and backward whirling is observed at the bearing and disk, respectively, between the critical speeds.

REFERENCES

1. A. Tondl 1965 *Some Problems of Rotor Dynamics*. London: Chapman and Hall.
2. F. M. Dimintberg 1961 *Flexural Vibrations of Rotating Shafts*. London: Butterworth.
3. J. S. Rao 1982 *Mechanisms and Machine Theory Journal* **17**, 143–152. Conditions for backward synchronous whirl of a flexible rotor in hydrodynamic bearings.
4. J. S. Rao 1991 *Rotor Dynamics* (second edition). New Delhi: Wiley Eastern.
5. J. S. Rao, R. B. Bhat and T. S. Sankar 1980–81 *Transactions of the Canadian Society of Mechanical Engineers* **6**, 155–161. A theoretical study of the effect of damping on the synchronous whirl of a rotor in hydrodynamic bearings.
6. C. Rajalingham, N. Ganesan and B. S. Prabhu 1986 *Journal of Sound and Vibration* **111**, 29–36. Conditions of backward whirling motion of a flexible rotor supported on hydrodynamic journal bearings.
7. R. Subbiah, R. B. Bhat, T. S. Sankar and J. S. Rao 1985 *NASA Conference Publication* 2409, *Proceedings of a Symposium sponsored by Bently Rotor Dynamics Research Corporation and held in Carson City*, *Nevada*, 145–154. Backward whirl in a simple rotor supported on hydrodynamic bearings.
8. C. Rajalingham, R. B. Bhat and V. K. Jha 1989 60*th Shock and Vibration Symposium*, Virginia Beach, 95–106. Simultaneous backward and forward whirling motion of disk and journal in a Jeffcott rotor supported on fluid film bearings.
9. C. Rao, R. B. Bhat and G. D. Xistris 1996 *Journal of Sound and Vibration* **198**, 379–388. Experimental verification of simultaneous forward and backward whirling at different points of a Jeffcott rotor supported on identical journal bearings.
10. C. Rao 1993 Ph.D. Thesis, Concordia University. Analytical and experimental investigation of the existence of simultaneous forward and backward whirling motion of a Jeffcott rotor supported on hydrodynamic bearings.

APPENDIX: NOMENCLATURE

$a_{xc}, a_{yc}, c_{xc}, c_{yc}$	cosine coefficients defined in equation (26) for rotor
a_{xl}, a_{yl}	cosine coefficients defined in equation (26) for left bearing
a_{xr}, a_{yr}	cosine coefficients defined in equation (26) for right bearing
b	bearing width
$b_{xc}, b_{yc}, d_{xc}, d_{yc}$	sine coefficients defined in equation (26) for rotor
b_{xl}, b_{yl}	sine coefficients defined in equation (26) for left bearing
b_{xr}, b_{yr}	sine coefficients defined in equation (26) for right bearing
c	clearance parameter, $c = (c_l + c_r)/2$
c_l	radial clearance at left bearing
$\bar{c}_l$	non-dimensional clearance ratio, $\bar{c}_l = c_l/c$
c_r	radial clearance at right bearing
$\bar{c}_r$	non-dimensional clearance ratio, $\bar{c}_r = c_r/c$
$C_{xx,l}, \ldots$	damping coefficients for left journal bearing
$\bar{C}_{xx,l}, \ldots$	non-dimensional damping coefficients, $\bar{C}_{xx,l} = C_{xx,l}c_l\omega/(W/2)$
$C_{xx,r}, \ldots$	damping coefficients for right journal bearing
d	diameter of journal
$\bar{C}_{xx,r}$	non-dimensional damping coefficients, $\bar{C}_{xx,r} = C_{xx,r}c_r\omega/(W/2)$
G_x, G_y	gyroscopic couple
J	polar moment of inertia
$\bar{J}$	$\bar{J} = J/ml^2$, non-dimensional polar moment of inertia
K_s	stiffness of shaft
$K_{xx,l}, \ldots$	stiffness coefficients for left journal
$\bar{K}_{xx,l}, \ldots$	$\bar{K}_{xx,l} = (K_{xx,l}c_l/W/2)$, non-dimensional stiffness coefficients
$K_{xx,r}, \ldots$	stiffness coefficients for right journal
$\bar{K}_{xx,r}, \ldots$	$\bar{K}_{xx,r} = (K_{xx,r}c_r/W/2)$, non-dimensional stiffness coefficients
l	length of shaft
m	mass of shaft
P_x, P_y	force components
$\bar{R}$	non-dimensional imbalance response
S_0	$(p_{av}\psi^2)/\eta\omega$, Sommerfeld number
So_0	load parameter, $So_0 = \{(Wb/d)\psi^2/(\eta\omega_0)\}$
W	bearing load, $W = (mg/2)$
δ_s	static deflection, $\delta_s = (mgl^3)/48EI$
η	coefficient of viscosity
ω	u/r, journal angular velocity
ω_0	$\omega_0 = (g/c)^{1/2}$
ω_s	$\omega_s = (K_s/m)^{1/2}$
μ_s	flexibility parameter, $\mu_s = (\omega_0^2/\omega_s^2); = \delta_s/c$
ψ	clearance ratio, $\psi = 2c/d$
(ξ_{xl}, ξ_{yl})	co-ordinates of left bearing
(ξ_{xr}, ξ_{yr})	co-ordinates of right bearing
(ξ_{xc}, ξ_{yc})	co-ordinates of disk
$(\bar{\xi}_{xl}, \bar{\xi}_{yl}); (\bar{\xi}_{xr}, \bar{\xi}_{yr})$	non-dimensional co-ordinates of journal
$\bar{\xi}_{\dot{x}l} \cdots$	$\bar{\xi}_{\dot{x}l} = (\xi_{xl} - \xi_{xlc})/c$
$\bar{\xi}_{\dot{x}l}$	$\bar{\xi}_{\dot{x}l} = \omega\bar{\xi}'_{xl}$
$\bar{\xi}_{\dot{y}l}$	$\bar{\xi}_{\dot{y}l} = \omega\bar{\xi}'_{yl}$
$\bar{\xi}_{xr} \cdots$	$\bar{\xi}_{xr} = (\xi_{xr} - \xi_{xrc})/c$
$(\bar{\xi}_{xc}, \bar{\xi}_{yc}); (\bar{\theta}_{xc}, \bar{\theta}_{yc})$	non-dimensional co-ordinates of disk
$\bar{\xi}_{xc} \cdots$	$\bar{\xi}_{xc} = (\xi_{xc} - \xi_{xco})/c$
$\bar{\theta}_{xc} \cdots$	$\bar{\theta}_{xc} = (1/c)(\theta_{xc} - \theta_{xco})$
θ_{xc}	$\mathrm{d}\xi_x/\mathrm{d}z$
θ_{yc}	$\mathrm{d}\xi_y/\mathrm{d}z$
δ_ς	rotor deflection at centre
$\bar{\xi}_{\dot{x}c}$	$\bar{\xi}_{\dot{x}c} = \omega\bar{\xi}''_{xc}$
$\bar{\xi}_{\dot{x}c}$	$\bar{\xi}_{\dot{x}c} = \dot{\xi}_{xc}/c$
$\bar{\xi}_{xc}$	$\bar{\xi}_{xc} = \omega^2\bar{\xi}''_{xc}$
$'$	differentiation with respect to ωt
$\cdot$	differentiation with respect to t